

# Thermal stress control of a two-stage steam turbine system via efficient NMPC strategies\*

Riccardo Bacci di Capaci

*Department Civil and Industrial Engineering  
University of Pisa  
Pisa, Italy  
riccardo.bacci@unipi.it*

Marco Vaccari

*Department Civil and Industrial Engineering  
University of Pisa  
Pisa, Italy  
marco.vaccari@unipi.it*

Gabriele Pannocchia

*Department Civil and Industrial Engineering  
University of Pisa  
Pisa, Italy  
gabriele.pannocchia@unipi.it*

**Abstract**—Steam turbines are one of the key components of thermal power units, and any additional improvement in their efficiency has an important economic significance. In the case of concentrated solar plants, the steam turbines experience rapid fluctuations in working conditions as they are subject to multiple start-ups that lead to considerable thermal stress in the rotor region. A two-stage system, comprised of a series of a high-pressure (HP) and a low-pressure (LP) turbine, is here investigated and optimized. The proposed nonlinear model predictive control (NMPC) algorithms have a two-fold objective, that is, the optimal regulation of the total generated electric power and the simultaneous limitation of thermal stress on both turbines. The proposed formulations incorporate time-varying constraints and nonlinear disturbances that fluctuate within the prediction horizon of the controller's dynamic module. A suitable collocation method is derived and compared with a traditional multiple-shooting approach. The adoption of slack variables is also investigated, but the peculiar benefits prove to be negatively compensated by higher computational times. As a final result, the collocation method without slacks demonstrates the most efficient solution to solve the considered optimal control problem.

**Index Terms**—Nonlinear model predictive control, Rotor stress control, Two-stage steam turbine system

## I. INTRODUCTION

Modern power plants must handle intermittent operations with high flexibility. Steam turbines used in modern power generation facilities, like Concentrated Solar Power Plants (CSPs) or Combined Cycle Power Plants (CCPPs), are more frequently affected by load changes than in traditional applications. These variations stem from site weather conditions in the CSP instance and by different plant operation scenarios (i.e., from base load to peak load follower) in the CCPP case.

This study examines a CSP plant, a key solar technology for current and future electricity needs [1]. CSPs generate power by using solar collectors to produce high-temperature steam,

which drives steam turbines (STs) that convert thermal energy into electricity. STs consist of multiple blade row pairs (stators and rotors) and typically operate at three pressure levelshigh (HP), medium (MP), and low (LP)each defined by specific steam pressure and temperature.

One major problem the STs in CSP plants suffer is linked to the start-up phase, during which the high-temperature gradient between steam (at the rotor skin) and the rotor core can induce mechanical stress and then damage the turbines (thus, named thermal stress). Therefore, with the primary goal of optimizing start-up phases [2], specific control methods have been researched and developed for limiting rotor stress [3]. Authors in [4] have shown the advantages of using an online block for rotor stress monitoring and a control technique based on Nonlinear Model Predictive Control (NMPC) has been put into practice [5]. However, the proposed Sequential Quadratic Programming (SQP) algorithm has a high computational burden, making it uncompetitive with proprietary nonlinear optimization solvers. This limited its use with commercial software and affected the economics of the project.

This paper aims at extending the results already reported in our recent work [6], where two different types of steam turbines (high and low pressure) were analyzed and controlled only separately. To this purpose, the whole two-stage steam turbine system is now investigated and optimized. This augmented case study requires significant computer resources due to its comprehensive nonlinear model and the various involved nonlinear disturbances which represent time-varying constraints on the outputs and the control action. The open-source MPC-code [7] is used as an algorithm; the core files are written in *Python* and use IPOPT as a nonlinear programming solver and CasADi as a symbolic framework.

The remainder of the paper is as follows: Section II details the various components of the adopted dynamic model while Section III describes the investigated optimization methods for control; Section IV presents the obtained results in closed-loop

\* This research was funded by the European Union under Horizon Europe Grant Agreement number 101079342 (Fostering Opportunities Towards Slovak Excellence in Advanced Control for Smart Industries).

simulations. Finally, conclusions are drawn in Section V.

## II. THE MODEL

First, the two-stage ST system is described. The mathematical model for the dynamics of the single two STs follows, covering rotor temperature and the associated thermal stress.

### A. Model description

A scheme of the considered two-stage steam turbine system is shown in Figure 1. High-pressure steam is produced within the concentrated solar plant and expanded in two consecutive steam turbines, high (HP) and low (LP) pressure, coupled by a gearbox system (GB). The following variables are considered:

- **2 inputs** ( $u$ ): the wheel chamber pressures, that is, the pressure of first-stage region of the two turbines ( $P_{wch}^{HP}$ ;  $P_{wch}^{LP}$ );
- **3 outputs** ( $y$ ): the rotor thermal stress on the two turbines,  $\sigma^{HP}$  and  $\sigma^{LP}$ , and the total generated electric power  $W$ , as the sum of two contributions:  $W = W^{HP} + W^{LP}$ ;
- $N_x$  **states** ( $x$ ): i.e., the rotor temperatures  $T$  for the two turbines, from the core to the skin, adopted in the spatial discretization.
- **6 external disturbances** ( $d$ ): the inlet steam pressures ( $P_{in}^{HP}$ ;  $P_{in}^{LP}$ ), the inlet steam temperatures ( $T_{steam}^{HP}$ ;  $T_{steam}^{LP}$ ), and the outlet steam pressures ( $P_{out}^{HP}$ ;  $P_{out}^{LP}$ ).

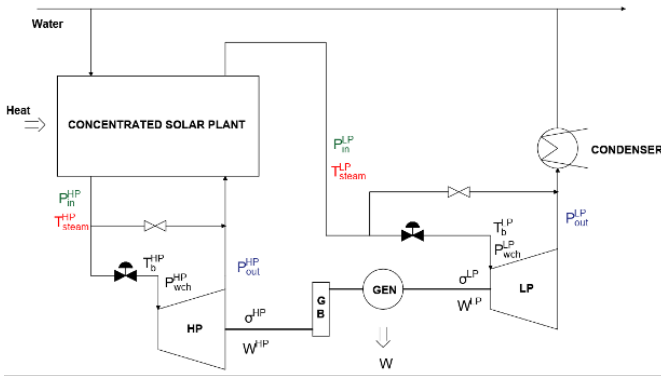


Fig. 1: Simplified scheme of the considered two-stage steam turbine system with the main variables.

### B. Thermal model

The following partial differential equation (PDE), which uses partial derivatives of temperature  $T$  with respect to time  $t$  and radius  $r$ , is used to characterize the thermal dynamics of the rotor of each steam turbine in cylindrical coordinates:

$$\rho C_p \frac{\partial T}{\partial t} = \frac{1}{r} \frac{\partial}{\partial r} \left( k r \frac{\partial T}{\partial r} \right) \quad (1)$$

A suitable initial condition and two boundary conditions apply for each turbine, written in general notation as follows:

$$\begin{cases} \frac{\partial T}{\partial r} \big|_{r=0} = 0 \\ -k \frac{\partial T}{\partial r} \big|_{r=R} = HTC(t)(T(t)|_{r=R} - T_b(t)) \end{cases} \quad (2)$$

where  $\rho$  is the density [ $\text{kg/m}^3$ ],  $C_p$  is the heat capacity [ $\text{J/(kg K)}$ ],  $HTC$  is the global heat transfer coefficient [ $\text{W/(m}^2 \text{K)}$ ], and  $k$  is the thermal conductivity [ $\text{W/(m K)}$ ] among the physical parameters of the two rotor steel. Lastly,  $R$ , that is,  $R^{HP}$  and  $R^{LP}$ , is the external rotor radius, and  $T_b$ , that is,  $T_b^{HP}$  and  $T_b^{LP}$ , is the bulk temperature, or the steam temperature pertinent to the two convection phenomena.

The spatial partial derivatives are then reduced to ordinary ones using an explicit finite difference approach once the radial domain has been uniformly discretized over  $N_r + 1$  nodes (that is,  $N_r^{HP} + 1$  and  $N_r^{LP} + 1$ ) for each turbine:

$$\frac{\partial T_i}{\partial r} = \frac{T_{i+1} - T_{i-1}}{2\Delta r}; \quad \frac{\partial^2 T_i}{\partial r^2} = \frac{T_{i+1} - 2T_i + T_{i-1}}{\Delta r^2} \quad (3)$$

with  $\Delta r = r_{i+1} - r_i$ . Thus, after a few steps, the following expression for the ordinary time derivative can be achieved:

$$\frac{dT_i}{dt} = \frac{k}{\rho C_p r_i} \frac{T_{i+1} - T_{i-1}}{2\Delta r} + \frac{k}{\rho C_p} \frac{T_{i+1} - 2T_i + T_{i-1}}{\Delta r^2} \quad (4)$$

Therefore, a system of ordinary differential equations (ODEs) is obtained, subject to the following two corrected boundary conditions, as reported in [8]:

$$\begin{cases} \frac{dT_0}{dt} = 4 \frac{k}{\rho C_p} \frac{T_1 - T_0}{\Delta r^2} \\ \frac{dT_{N_r}}{dt} = \frac{1}{\rho C_p} \frac{1}{R \Delta r^2} (0.5k_r(2R + \Delta r)(T_{N_r+1} - T_{N_r}) + 0.5k_l(R + r_{N_r-1})(T_{N_r-1} - T_{N_r})) \end{cases} \quad (5)$$

where  $T_{N_r+1}$  is the fictitious temperature evaluated as:

$$T_{N_r+1} = T_{N_r-1} - 2HTC \frac{\Delta r}{k_r} (T_{N_r} - T_b) \quad (6)$$

Note that all the physical properties are temperature-dependent;  $\rho$ ,  $k$ , and  $C_p$  are estimated with standard polynomial functions and are evaluated at the central temperature, i.e.  $T_i$ ;  $k_r$  is estimated at  $T_{N_r}$  and  $k_l$  at the mean temperature between  $T_{N_r}$  and  $T_{N_r-1}$ . The other variables, such as the heat transfer coefficient  $HTC$ , the bulk temperature  $T_b$ , and also the generated electric power  $W$  are described by empirical static functions of the measured variables, that is, the inlet and outlet steam pressure, the inlet steam temperature, and the wheel chamber pressure of each turbine, e.g.,  $HTC^{LP} = f(P_{in}^{LP}, P_{out}^{LP}, T_{steam}^{LP}, P_{wch}^{LP})$ . According to previously routine plant data [4], the corresponding coefficients are known.

### C. Stress model

The dynamic equivalent stress on the rotor's external surface can be estimated from the general expression of von Mises:

$$\sigma(t) = \left[ \frac{\beta E}{1 - \nu} \left( T(r, t)|_{r=R} - \frac{2}{R^2} \int_0^R T(r, t) r dr \right) \right] \quad (7)$$

where  $\beta$  is the thermal expansion coefficient [ $1/\text{C}$ ],  $E$  is the Young modulus [ $\text{MPa}$ ], and  $\nu$  is the Poisson ratio of the rotor steel. Standard polynomial functions of the rotor surface temperature are used to assess these physical parameters. Note that the following linear relation [9] can numerically approximate at any time instant  $j$  the integral term in Eq. (7):

$$\sigma^j = C \cdot T^j = [c_0 \quad \dots \quad c_{N_r}] [T_0 \dots T_{N_r}]_j' \quad (8)$$

where:

$$C = \frac{\beta E}{1 - \nu} \left[ -\frac{\Delta r^2}{R^2}, \quad -\frac{2r_1 \Delta r}{R^2}, \quad \dots \quad -\frac{2r_{N_r-1} \Delta r}{R^2}, \quad 1 - \frac{\Delta r}{R} \right]$$

### III. THE METHODS

The investigated NMPC problems are described below.

#### A. NMPC formulation

The original continuous-time problem is as follows:

$$\min_{x(\cdot), u(\cdot)} \int_0^\tau \ell_c(x(t), u(t)) dt \quad \text{s.t.} \quad (9a)$$

$$x(0) = x_0^* \quad (9b)$$

$$\dot{x} = f_c(x(t), u(t)) \quad (9c)$$

$$G(x(t), u(t), t) \leq 0 \quad (9d)$$

in which the objective function  $\ell_c(\cdot)$  is integrated over the prediction horizon  $\tau$ , from the initial state  $x_0^* \in R^{N_x}$  and subject to the inequality constraint function  $G(\cdot)$ . This function  $G(\cdot)$  includes, among the others, lower and upper bounds for the total electric power  $W$  and two nonlinear functions involving time-varying upper bounds for two terms of stress ( $\sigma_{ub}^{HP}(t)$ ,  $\sigma_{ub}^{LP}(t)$ ), suitably calculated, as detailed later.

a) *Standard multiple-shooting*: Problem (9) is discretized, which involves the integration of both the rotor thermal model  $f_c$  and objective function  $\ell_c$  over a finite number  $N$  of time steps. In this framework, one popular implementation of Problem (9) employs, as optimization variables, the sequences of states  $\mathbf{x} := (x_0, x_1, \dots, x_N)$  and control actions  $\mathbf{u} := (u_0, u_1, \dots, u_{N-1})$  simultaneously, describing the so-called *multiple shooting* method. The optimization problem is thus reformulated in discrete-time as follows:

$$\min_{\mathbf{x}, \mathbf{u}} \sum_{\kappa=0}^{N-1} \ell(x_\kappa, u_\kappa) \quad \text{s.t.} \quad (10a)$$

$$x_0 = x_0^* \quad (10b)$$

$$x_{\kappa+1} = F(x_\kappa, u_\kappa), \quad \kappa = 0, \dots, N-1 \quad (10c)$$

$$G(x_\kappa, u_\kappa, \kappa) \leq 0, \quad \kappa = 0, \dots, N-1 \quad (10d)$$

where  $F$  is the integrated state map from  $f_c$ , and  $\ell$  approximates the integral of  $\ell_c$  over each interval.

b) *Collocation method*: As a direct transcription technique, collocation methods use a polynomial function to approximate the continuous-time state trajectory, with coefficients determined alongside the control trajectory [10]. *Derivative* or *state* representation can be used, [11] and in this work, the state approach is adopted, introducing *internal states*  $S_\kappa$  as additional optimization variables. Suitable equality constraints  $H(\cdot)$  and a modified state update  $F_\kappa(\cdot)$  are employed to follow an implicit integration rule, where  $M = 2$  is the order of the integration method, that is, the fourth-order Gauss-Legendre method is adopted (see Ref. [6] for more details). Using a multiple shooting approach and adding optimization variables

$\mathbf{S} := (S_0, S_1, \dots, S_{N-1})$ , Problem (9) is reformulated as follows:

$$\min_{\mathbf{x}, \mathbf{S}, \mathbf{u}} \sum_{\kappa=0}^{N-1} \ell(x_\kappa, S_\kappa, u_\kappa) \quad \text{s.t.} \quad (11a)$$

$$x_0 = x_0^* \quad (11b)$$

$$x_{\kappa+1} = F_\kappa(x_\kappa, S_\kappa, u_\kappa), \quad \kappa = 0, \dots, N-1 \quad (11c)$$

$$H(x_\kappa, S_\kappa, u_\kappa) = 0, \quad \kappa = 0, \dots, N-1 \quad (11d)$$

$$G(x_\kappa, S_\kappa, u_\kappa, \kappa) \leq 0, \quad \kappa = 0, \dots, N-1 \quad (11e)$$

The transition to the next state is indeed performed through:

$$x_{\kappa+1} = F_\kappa(x_\kappa, S_\kappa, u_\kappa) := x_\kappa + \tilde{b}_1(s_{\kappa1} - x_\kappa) + \tilde{b}_2(s_{\kappa2} - x_\kappa) \quad (12)$$

where  $\tilde{b}$  derive from the Butcher tableau, as explained in [6]. Note that for the state update is not necessary to integrate the differential system in each iteration; hence, there is a considerable reduction in computational costs [12].

#### B. The optimization problem

Bounds on the control action  $u = [P_{wh}^{HP}, P_{wh}^{LP}]$  are set as:

$$\min(P_{in,\kappa}^{LP}, P_{out,\kappa}^{LP}) \leq P_{wh,\kappa}^{LP} \leq \max(P_{in,\kappa}^{LP}, P_{out,\kappa}^{LP}) \quad (13a)$$

$$\min(P_{in,\kappa}^{HP}, P_{out,\kappa}^{HP}) \leq P_{wh,\kappa}^{HP} \leq \max(P_{in,\kappa}^{HP}, P_{out,\kappa}^{HP}) \quad (13b)$$

$$\forall \kappa = 0, \dots, N-1$$

For the states ( $x$ ), i.e., the two rotor temperatures  $T$ , we set  $0 \geq T \geq T^{max}$ , where the maximum value is related to the maximum steam temperature registered during the normal system operation, that is,  $T^{max} = 1.05 \cdot \max(T_{steam})$ .

The inequality constraint function  $G(\cdot)$  includes:

- constant lower bound for each turbine contribution to the total electric power ( $W^{HP}$ ,  $W^{LP}$ );
- constant lower and upper bounds for the total power  $W$ ;
- constant upper bound for the difference between the two turbine contributions to the total power, that is,  $\Delta W_\kappa \leq \Delta W^{max}$ , where  $\Delta W_\kappa = |W_\kappa^{HP} - W_\kappa^{LP}|$ ;
- a time-varying upper bound on the thermal stress of two rotors, that is,  $\sigma_\kappa^{HP} \leq \sigma_\kappa^{HP,max}$  and  $\sigma_\kappa^{LP} \leq \sigma_\kappa^{LP,max}$ .

The stress upper bound for both turbines is computed as  $\sigma_\kappa^{max} = \sigma_{ten,\kappa} - \sigma_{cen}$ , where  $\sigma_{ten}$  and  $\sigma_{cen}$  are the tensile and centrifugal stress, respectively, with  $\sigma_{ten,\kappa}$  as a function of rotor skin temperature and, thus, time. When slack variables are included in the problem formulation, the following vector is set  $\epsilon = [\epsilon^1, \epsilon^2, \epsilon^3, \epsilon^4, \epsilon^5, \epsilon^6, \epsilon^7, \epsilon^8, \epsilon^9, \epsilon^{10}, \epsilon^{11}]$ , thus, the constraints are modified as in Eq (14):  $\epsilon^1$  and  $\epsilon^2$  soften the lower bounds on two contributions to the total power;  $\epsilon^3$  and  $\epsilon^4$  soften the constraint on the minimum and maximum total power  $W$ ;  $\epsilon^5$  softens the constraint on the difference between the two power contributions;  $\epsilon^6$ ,  $\epsilon^7$  soften the constraint on the two components of maximum stress;  $\epsilon^8 - \epsilon^{11}$  soften the bound constraints on the control action. Note that a constraint on the maximum total power  $W^{max}$  is to include eventual limitations in the gearbox or to simulate the presence of an external override system.

$$W_{\kappa}^{HP} \geq W_{\kappa}^{HP,min} - \epsilon^1 \quad (14a)$$

$$W_{\kappa}^{LP} \geq W_{\kappa}^{LP,min} - \epsilon^2 \quad (14b)$$

$$W_{\kappa} \geq W_{\kappa}^{min} - \epsilon^3 \quad (14c)$$

$$W_{\kappa} \leq W_{\kappa}^{max} + \epsilon^4 \quad (14d)$$

$$\Delta W_{\kappa} \leq \Delta W_{\kappa}^{max} + \epsilon^5 \quad (14e)$$

$$\sigma_{\kappa}^{HP} \leq \sigma_{\kappa}^{HP,max} + \epsilon^6 \quad (14f)$$

$$\sigma_{\kappa}^{LP} \leq \sigma_{\kappa}^{LP,max} + \epsilon^7 \quad (14g)$$

$$P_{wch,\kappa}^{HP} \geq P_{wch,\kappa}^{HP,min} - \epsilon^8 \quad (14h)$$

$$P_{wch,\kappa}^{HP} \leq P_{wch,\kappa}^{HP,max} + \epsilon^9 \quad (14i)$$

$$P_{wch,\kappa}^{LP} \geq P_{wch,\kappa}^{LP,min} - \epsilon^{10} \quad (14j)$$

$$P_{wch,\kappa}^{LP} \leq P_{wch,\kappa}^{LP,max} + \epsilon^{11} \quad (14k)$$

Note that slack variables ensure feasibility by preventing the optimization from avoiding infeasible regions, which could otherwise cause significant stress violations. This approach allows for minor temporary stress-bound breaches but ensures a quick recovery. A more detailed discussion on their impact will follow in the results Section. For simplicity, fixed slack values along the prediction horizon are assumed, reflecting the maximum violation of the corresponding constraint. If non-fixed slack variables were adopted, the dimensionality of  $\epsilon$  would increase, i.e.,  $\epsilon \in R^{11 \times N}$ , impacting computational costs.

In addition, constant hard constraints are imposed on the input variation, as follows:

$$\Delta P_{wch}^{HP,min} \leq \Delta P_{wch,\kappa}^{HP} \leq \Delta P_{wch}^{HP,max} \quad (15a)$$

$$\Delta P_{wch}^{LP,min} \leq \Delta P_{wch,\kappa}^{LP} \leq \Delta P_{wch}^{LP,max} \quad (15b)$$

Note that given the peculiar problem framework where the variation of the control action  $\Delta u$  significantly impacts stress levels, having these two constraints as soft could offer an additional lever for manipulation. Nevertheless, by incorporating  $\Delta u$  into the objective function with appropriate weighting, we may achieve good performance without the use of additional slack, which may further increase the computational burden.

Also note that since the difference between the power contributions given by the two turbines can be high (i.e.,  $\Delta W^{max} = 30$  MW), a relatively small negative lower bound ( $W^{HP/LP,min} = -1$  MW) has been assigned to allow the turbine to temporarily absorb power and operate as a motor device. As a matter of fact, in open-loop simulations of high-pressure turbine [6], the empirical function for variable  $W$  proves to assume negative values when  $P_{out}^{HP} > P_{in}^{HP}$ , but also when  $P_{in}^{HP} - P_{out}^{HP} < \Delta P = 1.15$  bar. Nevertheless, the lower bound on the total power is set as positive ( $W^{min} = 0$  MW) to ensure continuous electricity generation.

### C. Features

Below is a brief description of the specific parameters adopted and the modules composing the algorithm.

- **Steady-state Optimization:** the adopted objective function is quadratic and minimizes the square deviation of

the output target ( $y_s$ ) from its set-points ( $y_{sp}$ ), weighted by the cost matrix  $Q_{ss}$ :

$$\bar{\ell} = \frac{1}{2}(y_s - y_{sp})^T Q_{ss}(y_s - y_{sp}) \quad (16)$$

- **Dynamic Optimization:** the difference between the actual and set-point values ( $y_{sp}$ ) of the output  $y = F_y(x, u, d)$ , weighted by the matrix  $Q$ , as well as the input variations by matrix  $S$  and the slack variables  $\epsilon$  by matrix  $W_s$ , over horizon  $N$  is considered as follows:

$$\frac{1}{N} \sum_{\kappa=0}^{N-1} \ell(x_{\kappa}, u_{\kappa}) = \frac{1}{N} \sum_{\kappa=0}^{N-1} [(y_{\kappa} - y_{sp})^T Q (y_{\kappa} - y_{sp}) + (u_{\kappa} - u_{\kappa-1})^T S (u_{\kappa} - u_{\kappa-1})] + \epsilon^T W_s \epsilon \quad (17)$$

where  $u_{-1}$  is known. As a starting point for tuning, we adopted values previously used for simulations performed on the two single turbines [6]. After further refinement, we finally set  $N = 30$ ,  $Q_{ss} = Q = \text{diag}(0, 0, 1)$ ,  $S = \text{diag}(60, 60)$ . Note that since tracking a set-point for the two terms of stress is not necessary, a good choice of parameters in  $Q$  enables the power to follow its reference. At the same time, the influence of matrix  $S$  guarantees limited fluctuations of manipulated variables, avoiding needless strain on the two control valves.

To improve the solver performance, calibrated weight values for the different slack variables are set, that is,  $W_s = \text{diag}(w_{s1}, \dots, w_{s11})$ . The main idea is to give priority to fulfilling the constraint on the power bounds while reducing the weight on the violation of the stress limits. In other words, the two stress limits can be exceeded if doing so proves beneficial to avoid entering regions where the turbines performance becomes unrealistic in terms of power generation.

## IV. RESULTS

MPC-code aims to be as general a resource as feasible, thus it is constantly being updated<sup>1</sup>. To this aim, the version currently accessible on *GitHub* incorporates all the appropriate modifications made for the analysis of the present case study.

The following closed-loop simulations are executed by exploiting data registered from an industrial two-stage steam turbine system; in particular, real data for  $P_{in}^{HP/LP}$ ,  $T_{steam}^{HP/LP}$ ,  $P_{out}^{HP/LP}$  are treated as six external disturbances and let vary across the prediction horizon of our controllers. Note that this challenging scenario intends to emulate a typical industrial start-up and is well-suited to validate the developed formulations of NMPCs. Note also that the considered simulation is a nominal scenario, with no plant/model mismatch and no requirement for a disturbance model [11].

### A. Discussion

The solution obtained from the traditional multiple shooting (MS) approach, as in (10), is compared with the one derived using the collocation method, as in (11), with (CM-SI) and without (CM) the adoption of slack variables. As a general result, it is worth noting that the responses obtained for the

<sup>1</sup><https://github.com/CPCLAB-UNIP/MPC-code/wiki>

three tested methods are comparable. As an example, Figure 2 shows the time trends obtained with the collocation method (CM). The results of the other two methods are not reported for the sake of brevity. Note also that numerical values of variables on the y-axis are omitted for privacy reasons.

As shown by Figure 2, the controller can achieved the required trade-off: keep the thermal stress under its upper bound for both turbines and track the total power set-point with sufficient performance. Note that the optimization task is particularly challenging from 2100 seconds when  $P_{wh}^{HP}$  is very constrained, as  $P_{out}^{HP}$  tends to  $P_{in}^{LP}$ , until a scenario of pressure inversion around 2300s. The two contributions to total power are shown in the last panel of Figure 2. It is evident how the actual total power  $W$  can reach the steady-state value of the power ( $W_s$ ), but leaves an offset on the set-point ( $W_{sp}$ ) which is higher and proves not feasible. Note also that  $W_s$ , after an initial decrease at around 2300s, rapidly increases as if no stress bound is touched. This is because the stress results from the dynamics described by the rotor temperatures and relative gradients. It is therefore clear that at steady-state, at which all temperatures collide to one value, no stress can damage the turbines. It is also worth noting that  $W^{HP} < 0$  from 2100 to 2400s when  $P_{out}^{HP}$  is close to  $P_{in}^{HP}$ ; in this phase, the HP turbine absorbs power and operates as a motor device. To quantify the differences in responses of three different adopted methods, the Normalized Root Mean Square Error (NRMSE) between corresponding signals is computed:

$$NRMSE = \frac{1}{y^{M1}} \sqrt{\frac{1}{N_s} \sum_{\kappa=0}^{N_s} (y_{\kappa}^{M1} - y_{\kappa}^{M2})^2} \quad (18)$$

where  $y_k$  are the values of the generic variable obtained by method 1 (M1) and method 2 (M2),  $y^{M1}$  is the mean value for M1, and  $N_s$  is the number of samples. The numerical values for two input variables ( $P_{wh}^{HP}$ ,  $P_{wh}^{LP}$ ), the three outputs ( $\sigma^{HP}$ ,  $\sigma^{LP}$ ,  $W$ ), and the skin temperature of two rotors ( $T_{sk}^{HP}$  and  $T_{sk}^{LP}$ ) are shown in Table I.

Since the largest value between CM and MS, related to  $P_{wh}^{HP}$  and  $P_{wh}^{LP}$ , is around  $5 \cdot 10^{-6}$ , means that the developed collocation method proves to be an excellent approximation of the solution obtained with the traditional multiple shooting approach. This result confirms what was already found in [6] for a much simpler case study. In addition, since differences between CM and CM-SI are smaller than  $10^{-3}$ , the use of slack proves to not alter significantly the response. In particular, the improvement in performance in terms of tracking of  $W$  is pretty limited.

When slack variables are adopted, larger constraint violations on two terms of stress are observed, as illustrated by Figure 3. Nevertheless, note that in the case of CM, the obtained infeasibility is sparse and of moderate extent on the two terms of stress, that is, 58 occurrences out of 2700 samples, and an amplitude equal to a relative violation smaller than 0.05%, which is close to the set value of constraint tolerance. Therefore, the considered case study proves a scenario not particularly suited for the use of slack variables.

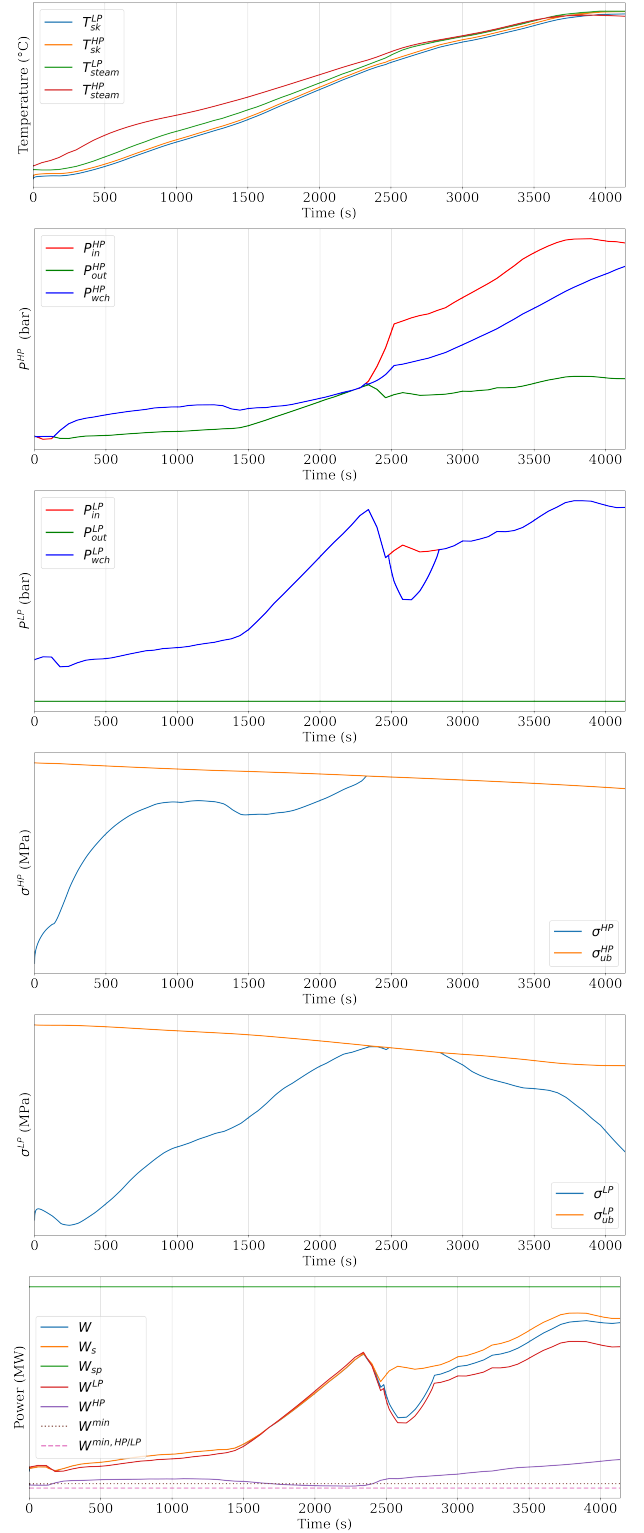


Fig. 2: Time trends obtained with collocation method (without slack variables).

The computational time required by the three methods is another important aspect. Simulations were performed on a MacBook Pro Apple M1 2021, 32 GB RAM. In particular,

TABLE I: Deviation in the responses: multiple shooting vs. collocation method.

$NRMSE$	$P_{wh}^{HP}$	$P_{wh}^{LP}$	$\sigma^{HP}$	$\sigma^{LP}$	$W$	$T_{sk}^{HP}$	$T_{sk}^{LP}$
MS vs. CM: ( $\times 10^6$ )	5.12	5.03	2.12	2.82	2.57	2.21	2.15
CM vs. CM-SI: ( $\times 10^5$ )	7.90	117.6	5.31	12.1	135.2	1.30	1.7

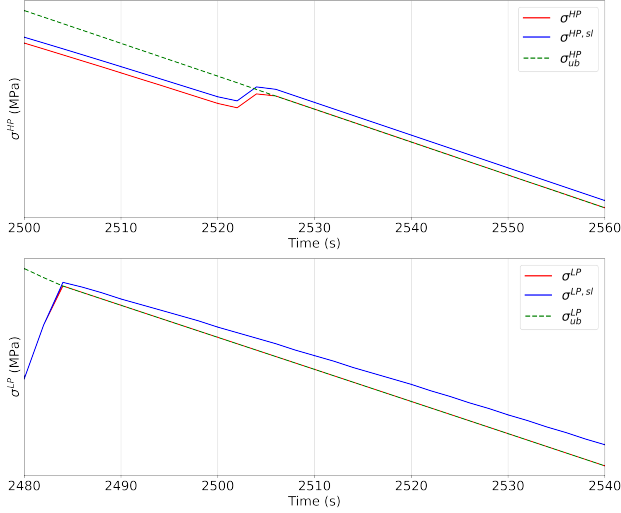


Fig. 3: Comparing trends of rotor stress on two turbines: collocation method with and without the use of slacks.

TABLE II: Computational times for different methods.

Method	Min [s]	Max [s]	Mean [s]	Std Dev [s]
MS	10.96	71.80	15.37	5.36
CM	0.42	1.03	0.65	0.156
CM-SI	1.20	1.67	1.35	0.072

the times per iteration (minimum, maximum, mean values and corresponding standard deviations) are reported in Table II. A significant reduction of mean computation time is obtained by the proposed two solutions of collocation methods: 96% for CM and 91% for CM-SI with respect to the traditional MS approach. Therefore, the CM demonstrates the only solution implementable online since the control sampling time is equal to 2 seconds. Note that, while computation time is significantly reduced, move-blocking techniques have not been considered in this study but could be explored in future work for further efficiency improvements. To sum up, all three designed NMPCs can guarantee the limitation of the thermal stress of the two rotors and also track the total power set-point. In addition, the use of slack variables does not particularly benefit the controller's performance for the specific case study. Note that this last observation cannot be considered general, as analyzing different start-up scenarios may lead to different conclusions about the adoption of soft constraints.

## V. CONCLUSION

In this work, we investigated efficient solutions of NMPC for steam turbines in concentrated solar systems. A two-stage system comprised of a high-pressure and a low-pressure

turbine represents a very realistic industrial scenario, more involved with respect to our previous work where the two turbines were optimized separately. The ultimate objective is well achieved: total electric power is regulated to target while physical constraints on the wheel chamber pressure and rotor thermal stress of both machines are respected, even in the face of time-varying operating conditions. The developed collocation method proves to significantly reduce computational costs for the dynamic optimization problem while yielding results that are close to those from a traditional multiple-shooting method.

## ACKNOWLEDGMENT

This work was possible thanks to the previous collaboration with the people of Baker Hughes, Firenze, Italy. We are very grateful to Eng.s Annamaria Signorini, Silvia Manara, and Federico Bucciarelli, for their fruitful discussions and sharing of process information and data of the system under investigation. We also sincerely thank Vittoria Garrucciu, as this new paper is based on her valuable work at UNIPI.

## REFERENCES

- [1] D. A. Baharoon, H. A. Rahman, W. Z. W. Omar, and S. O. Fadhil, "Historical development of concentrating solar power technologies to generate clean electricity efficiently: a review," *Renewable and Sustainable Energy Reviews*, vol. 41, pp. 996–1027, 2015.
- [2] D. Faillie and F. Davelaar, "Model based start-up optimization of a combined cycle power plant," *IFAC Proceedings Volumes*, vol. 42, no. 9, pp. 197–202, 2009, 6th IFAC CPES.
- [3] M. Banaszkiwicz, "On-line monitoring and control of thermal stresses in steam turbine rotors," *Appl. Therm. Eng.*, vol. 94, pp. 763–776, 2016.
- [4] F. Bucciarelli, D. Checcacci, G. Girezzi, and A. Signorini, "Operation and maintenance improvements of steam turbines subject to frequent start by rotor stress monitoring," in *GT2020. Proceedings of ASME Turbo Expo 2020*, vol. 9, p. V009T23A026.
- [5] S. Dettori, A. Maddaloni, F. Galli, V. Colla, F. Bucciarelli, D. Checcacci, and A. Signorini, "Steam turbine rotor stress control through nonlinear model predictive control," *Energies*, vol. 14, no. 13, 2021.
- [6] V. Garrucciu, R. Bacci di Capaci, M. Vaccari, S. Manara, F. Bucciarelli, A. Signorini, and G. Pannocchia, "Efficient nmpe strategies for thermal stress control of steam turbines," *IFAC-PapersOnLine*, vol. 58, no. 18, pp. 29–34, 2024, 8th IFAC Conf. on Nonlinear Model Predictive Control.
- [7] M. Vaccari, R. Bacci di Capaci, A. Busoni, and G. Pannocchia, "Easy-to-use MPC tool for controlling chemical processes in a rigorous simulation environment," *IFAC-PapersOnLine*, vol. 56, no. 2, pp. 2707–2712, 2023, 22nd IFAC World Congress.
- [8] A. Nakai, M. Nakamoto, A. Kakehi, and S. Hayashi, "Turbine start-up algorithm based on prediction of rotor thermal stress," in *Proc. of the 34th SICE Annual Conf., Inter. Session Papers*, 1995, pp. 1561–1564.
- [9] A. Rusin, G. Nowak, and M. Lipka, "Practical algorithms for online thermal stress calculations and heating process control," *Journal of Thermal Stresses*, vol. 37, no. 11, pp. 1286–1301, 2014.
- [10] P. Puchaud, F. Bailly, and M. Begon, "Direct multiple shooting and direct collocation perform similarly in biomechanical predictive simulations," *Comput. Methods Appl. Mech. Eng.*, vol. 414, p. 116162, 2023.
- [11] J. B. Rawlings, D. Q. Mayne, and M. Diehl, *Model Predictive Control: Theory, Computation, and Design*, 2nd Ed. Nob Hill Publishing, 2019.
- [12] Y. Song, B. Pan, Q. Fan, and B. Xu, "A computationally efficient sequential convex programming using chebyshev collocation method," *Aerospace Science and Technology*, vol. 141, p. 108584, 2023.